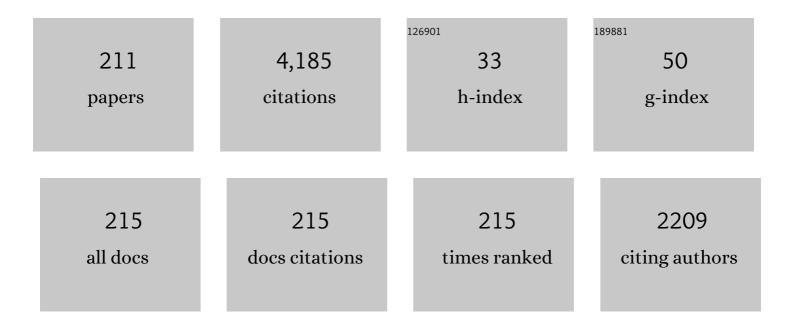
List of Publications by Year in descending order

Source: https://exaly.com/author-pdf/3493306/publications.pdf Version: 2024-02-01



#	Article	IF	CITATIONS
1	Simulation study on fundamental properties of the storm-time ring current. Journal of Geophysical Research, 2000, 105, 15843-15859.	3.3	181
2	Energetic electron precipitation associated with pulsating aurora: EISCAT and Van Allen Probe observations. Journal of Geophysical Research: Space Physics, 2015, 120, 2754-2766.	2.4	133
3	Formation process of relativistic electron flux through interaction with chorus emissions in the Earth's inner magnetosphere. Journal of Geophysical Research: Space Physics, 2015, 120, 9545-9562.	2.4	98
4	Numerical Simulation of the Ring Current: Review. Space Science Reviews, 2003, 105, 377-452.	8.1	84
5	Ring current and the magnetosphere-ionosphere coupling during the superstorm of 20 November 2003. Journal of Geophysical Research, 2005, 110, .	3.3	78
6	Structures of dayside whistlerâ€mode waves deduced from conjugate diffuse aurora. Journal of Geophysical Research: Space Physics, 2013, 118, 664-673.	2.4	76
7	Relation between fine structure of energy spectra for pulsating aurora electrons and frequency spectra of whistler mode chorus waves. Journal of Geophysical Research: Space Physics, 2015, 120, 7728-7736.	2.4	73
8	Temporal and Spatial Evolutions of a Large Sunspot Group and Great Auroral Storms Around the Carrington Event in 1859. Space Weather, 2019, 17, 1553-1569.	3.7	68
9	Generation region of pulsating aurora obtained simultaneously by the FAST satellite and a Syowa-Iceland conjugate pair of observatories. Journal of Geophysical Research, 2004, 109, .	3.3	67
10	Defining and resolving current systems in geospace. Annales Geophysicae, 2015, 33, 1369-1402.	1.6	66
11	Counter equatorial electrojet and overshielding after substorm onset: Global MHD simulation study. Journal of Geophysical Research: Space Physics, 2014, 119, 7281-7296.	2.4	65
12	Statistical distribution of the storm-time proton ring current: POLAR measurements. Geophysical Research Letters, 2002, 29, 30-1-30-4.	4.0	61
13	Modeling of solar wind control of the ring current buildup: A case study of the magnetic storms in April 1997. Geophysical Research Letters, 1998, 25, 3751-3754.	4.0	59
14	Postmidnight storm-time enhancement of tens-of-keV proton flux. Journal of Geophysical Research, 2004, 109, .	3.3	57
15	Chorus wave scattering responsible for the Earth's dayside diffuse auroral precipitation: A detailed case study. Journal of Geophysical Research: Space Physics, 2014, 119, 897-908.	2.4	56
16	Penetration of the convection and overshielding electric fields to the equatorial ionosphere during a quasiperiodic <i>DP</i> 2 geomagnetic fluctuation event. Journal of Geophysical Research, 2010, 115, .	3.3	55
17	Fate of outflowing suprathermal oxygen ions that originate in the polar ionosphere. Journal of Geophysical Research, 2006, 111, .	3.3	54
18	Global IMAGE/HENA observations of the ring current: Examples of rapid response to IMF and ring current-plasmasphere interaction. Journal of Geophysical Research, 2002, 107, SMP 12-1.	3.3	53

#	Article	IF	CITATIONS
19	Influence of ionosphere conductivity on the ring current. Journal of Geophysical Research, 2004, 109,	3.3	49
20	Long-lasting Extreme Magnetic Storm Activities in 1770 Found in Historical Documents. Astrophysical Journal Letters, 2017, 850, L31.	8.3	49
21	GPS phase scintillation associated with optical auroral emissions: First statistical results from the geographic South Pole. Journal of Geophysical Research: Space Physics, 2013, 118, 2490-2502.	2.4	45
22	East Asian observations of low-latitude aurora during the Carrington magnetic storm. Publication of the Astronomical Society of Japan, 0, , .	2.5	44
23	Low-latitude Aurorae during the Extreme Space Weather Events in 1859. Astrophysical Journal, 2018, 869, 57.	4.5	44
24	Dayside Magnetospheric and Ionospheric Responses to a Foreshock Transient on 25 June 2008: 2. 2â€Ð Evolution Based on Dayside Auroral Imaging. Journal of Geophysical Research: Space Physics, 2018, 123, 6347-6359.	2.4	44
25	The Great Space Weather Event during 1872 February Recorded in East Asia. Astrophysical Journal, 2018, 862, 15.	4.5	44
26	Twoâ€dimensional observations of overshielding during a magnetic storm by the Super Dual Auroral Radar Network (SuperDARN) Hokkaido radar. Journal of Geophysical Research, 2008, 113, .	3.3	41
27	Sheared flows and smallâ€scale Alfvén wave generation in the auroral acceleration region. Geophysical Research Letters, 2009, 36, .	4.0	41
28	Impacts of Magnetosheath High‧peed Jets on the Magnetosphere and Ionosphere Measured by Optical Imaging and Satellite Observations. Journal of Geophysical Research: Space Physics, 2018, 123, 4879-4894.	2.4	41
29	Wedge-like dispersion of sub-keV ions in the dayside magnetosphere: Particle simulation and Viking observation. Journal of Geophysical Research, 2001, 106, 29571-29584.	3.3	40
30	Possible Cause of Extremely Bright Aurora Witnessed in East Asia on 17 September 1770. Space Weather, 2017, 15, 1373-1382.	3.7	39
31	Substorm simulation: Insight into the mechanisms of initial brightening. Journal of Geophysical Research: Space Physics, 2015, 120, 7270-7288.	2.4	38
32	Substorm simulation: Formation of westward traveling surge. Journal of Geophysical Research: Space Physics, 2015, 120, 10,466.	2.4	37
33	The Extreme Space Weather Event in 1903 October/November: An Outburst from the Quiet Sun. Astrophysical Journal Letters, 2020, 897, L10.	8.3	36
34	CME front and severe space weather. Journal of Geophysical Research: Space Physics, 2014, 119, 10,041.	2.4	35
35	Visualization of rapid electron precipitation via chorus element wave–particle interactions. Nature Communications, 2019, 10, 257.	12.8	35
36	The extreme space weather event in September 1909. Monthly Notices of the Royal Astronomical Society, 2019, 484, 4083-4099.	4.4	35

#	Article	IF	CITATIONS
37	Multiple discrete-energy ion features in the inner magnetosphere: 9 February 1998, event. Annales Geophysicae, 2004, 22, 1297-1304.	1.6	34
38	Nonlinear impact of plasma sheet density on the storm-time ring current. Journal of Geophysical Research, 2005, 110, .	3.3	34
39	Magnetic coupling of the ring current and the radiation belt. Journal of Geophysical Research, 2008, 113, .	3.3	34
40	Quasi-stationary auroral patches observed at the South Pole Station. Journal of Geophysical Research, 2007, 112, n/a-n/a.	3.3	33
41	The Energization and Radiation in Geospace (ERG) Project. Geophysical Monograph Series, 0, , 103-116.	0.1	33
42	Rapid decay of storm time ring current due to pitch angle scattering in curved field line. Journal of Geophysical Research, 2011, 116, .	3.3	32
43	Dynamical property of storm time subauroral rapid flows as a manifestation of complex structures of the plasma pressure in the inner magnetosphere. Journal of Geophysical Research, 2009, 114, .	3.3	31
44	Historical Auroras in the 990s: Evidence of Great Magnetic Storms. Solar Physics, 2017, 292, 1.	2.5	30
45	Effects of a Weak Intrinsic Magnetic Field on Atmospheric Escape From Mars. Geophysical Research Letters, 2018, 45, 9336-9343.	4.0	29
46	Dynamic Inner Magnetosphere: A Tutorial and Recent Advances. , 2011, , 145-187.		28
47	A scheme for forecasting severe space weather. Journal of Geophysical Research: Space Physics, 2017, 122, 2824-2835.	2.4	28
48	Response of the magnetospheric convection to sudden interplanetary magnetic field changes as deduced from the evolution of partial ring currents. Journal of Geophysical Research, 2002, 107, SMP 1-1.	3.3	27
49	Generation of fieldâ€aligned current (FAC) and convection through the formation of pressure regimes: Correction for the concept of Dungey's convection. Journal of Geophysical Research: Space Physics, 2016, 121, 8695-8711.	2.4	27
50	Time Domain Simulation of Geomagnetically Induced Current (GIC) Flowing in 500â€kV Power Grid in Japan Including a Threeâ€Dimensional Ground Inhomogeneity. Space Weather, 2018, 16, 1946-1959.	3.7	27
51	Global simulation study for the time sequence of events leading to the substorm onset. Journal of Geophysical Research: Space Physics, 2017, 122, 6210-6239.	2.4	26
52	A great space weather event in February 1730. Astronomy and Astrophysics, 2018, 616, A177.	5.1	26
53	Temporal and spatial evolution of discrete auroral arcs as seen by Cluster. Annales Geophysicae, 2005, 23, 2531-2557.	1.6	25
54	Records of sunspots and aurora candidates in the Chinese official histories of the <i>Yuán</i> and <i>MÃng</i> dynasties during 1261–1644. Publication of the Astronomical Society of Japan, 2017, 69, .	2.5	25

#	Article	IF	CITATIONS
55	Development of low-cost multi-wavelength imager system for studies of aurora and airglow. Polar Science, 2020, 23, 100501.	1.2	25
56	Storm-time magnetic configurations at geosynchronous orbit: Comparison between the main and recovery phases. Journal of Geophysical Research, 2007, 112, n/a-n/a.	3.3	24
57	Coordinated EISCAT Svalbard radar and Reimei satellite observations of ion upflows and suprathermal ions. Journal of Geophysical Research, 2008, 113, .	3.3	24
58	Microscopic Observations of Pulsating Aurora Associated With Chorus Element Structures: Coordinated Arase Satelliteâ€PWING Observations. Geophysical Research Letters, 2018, 45, 12,125.	4.0	24
59	New Diagnosis for Energy Flow From Solar Wind to Ionosphere During Substorm: Global MHD Simulation. Journal of Geophysical Research: Space Physics, 2019, 124, 360-378.	2.4	24
60	Direct comparison of pulsating aurora observed simultaneously by the FAST satellite and from the ground at Syowa. Geophysical Research Letters, 2002, 29, 37-1.	4.0	23
61	Quiet-time mid-latitude trough: influence of convection, field-aligned currents and proton precipitation. Annales Geophysicae, 2005, 23, 3277-3288.	1.6	23
62	Tracing geomagnetic conjugate points using exceptionally similar synchronous auroras. Geophysical Research Letters, 2005, 32, .	4.0	23
63	Observations of veryâ€lowâ€energy (<10 eV) ion outflows dominated by O <sup>+</sup> ions in the region of enhanced electron density in the polar cap magnetosphere during geomagnetic storms. Journal of Geophysical Research, 2010, 115, .	3.3	23
64	Hemispheric asymmetry of the structure of dayside auroral oval. Geophysical Research Letters, 2014, 41, 8696-8703.	4.0	23
65	Formation of the Sunâ€aligned arc region and the void (polar slot) under the nullâ€separator structure. Journal of Geophysical Research: Space Physics, 2017, 122, 4102-4116.	2.4	23
66	Measurement of geomagnetically induced current (GIC) around Tokyo, Japan. Earth, Planets and Space, 2021, 73, .	2.5	22
67	Substorm simulation: Quiet and Nâ€5 arcs preceding auroral breakup. Journal of Geophysical Research: Space Physics, 2016, 121, 1201-1218.	2.4	21
68	Pulsating proton aurora caused by rising tone Pc1 waves. Journal of Geophysical Research: Space Physics, 2016, 121, 1608-1618.	2.4	21
69	Magnetosheath variations during the storm main phase on 20 November 2003: Evidence for solar wind density control of energy transfer to the magnetosphere. Geophysical Research Letters, 2005, 32, .	4.0	20
70	Source location of the wedge-like dispersed ring current in the morning sector during a substorm. Journal of Geophysical Research, 2006, 111, .	3.3	20
71	Fundamental properties of substorm time energetic electrons in the inner magnetosphere. Journal of Geophysical Research: Space Physics, 2013, 118, 1589-1603.	2.4	20
72	Energy Flow Exciting Fieldâ€Aligned Current at Substorm Expansion Onset. Journal of Geophysical Research: Space Physics, 2017, 122, 12,288.	2.4	20

5

#	Article	IF	CITATIONS
73	The 2â€Ð Structure of Foreshockâ€Driven Field Line Resonances Observed by THEMIS Satellite and Groundâ€Based Imager Conjunctions. Journal of Geophysical Research: Space Physics, 2019, 124, 6792-6811.	2.4	20
74	Short-period gravity waves and ripples in the South Pole mesosphere. Journal of Geophysical Research, 2011, 116, .	3.3	19
75	Earliest datable records of aurora-like phenomena in the astronomical diaries from Babylonia. Earth, Planets and Space, 2016, 68, 195.	2.5	19
76	The earliest drawings of datable auroras and a two-tail comet from the Syriac Chronicle of Zūqnīn. Publication of the Astronomical Society of Japan, 2017, 69, .	2.5	18
77	Discovery of 1ÂHz Range Modulation of Isolated Proton Aurora at Subauroral Latitudes. Geophysical Research Letters, 2018, 45, 1209-1217.	4.0	18
78	Intensity and time series of extreme solar-terrestrial storm in 1946 March. Monthly Notices of the Royal Astronomical Society, 2020, 497, 5507-5517.	4.4	18
79	Coulomb lifetime of the ring current ions with time varying plasmasphere. Earth, Planets and Space, 1998, 50, 371-382.	2.5	17
80	Empirical model of proton fluxes in the equatorial inner magnetosphere: 2. Properties and applications. Journal of Geophysical Research, 2003, 108, .	3.3	17
81	ERG – A small-satellite mission to investigate the dynamics of the inner magnetosphere. Advances in Space Research, 2006, 38, 1861-1869.	2.6	17
82	Dynamic variations of a convection flow reversal in the subauroral postmidnight sector as seen by the SuperDARN Hokkaido HF radar. Geophysical Research Letters, 2007, 34, .	4.0	17
83	A method for estimating the ring current structure and the electric potential distribution using energetic neutral atom data assimilation. Journal of Geophysical Research, 2008, 113, .	3.3	17
84	What caused the rapid recovery of the Carrington storm?. Earth, Planets and Space, 2015, 67, .	2.5	17
85	Records of sunspot and aurora activity during 581–959 CE in Chinese official histories concerning the periods of <i>SuĂ</i> , <i>Táng</i> , and the Five Dynasties and Ten Kingdoms. Publication of the Astronomical Society of Japan, 2017, 69, .	2.5	17
86	The Earliest Candidates of Auroral Observations in Assyrian Astrological Reports: Insights on Solar Activity around 660 BCE. Astrophysical Journal Letters, 2019, 884, L18.	8.3	17
87	Do the Chinese Astronomical Records Dated AD 776 January 12/13 Describe an Auroral Display or a Lunar Halo? A Critical Re-examination. Solar Physics, 2019, 294, 1.	2.5	16
88	Occurrence of great magnetic storms on 6–8 March 1582. Monthly Notices of the Royal Astronomical Society, 2019, 487, 3550-3559.	4.4	16
89	South American auroral reports during the Carrington storm. Earth, Planets and Space, 2020, 72, .	2.5	16
90	Geospace storm processes coupling the ring current, radiation belt and plasmasphere. Geophysical Monograph Series, 2005, , 207-220.	0.1	15

#	Article	IF	CITATIONS
91	Effect of R2â€FAC development on the ionospheric electric field pattern deduced by a global ionospheric potential solver. Journal of Geophysical Research, 2012, 117, .	3.3	15
92	The role of interplanetary shock orientation on SC/SI rise time and geoeffectiveness. Advances in Space Research, 2017, 59, 1425-1434.	2.6	15
93	Prediction of geomagnetically induced currents (GICs) flowing in Japanese power grid for Carrington-class magnetic storms. Earth, Planets and Space, 2021, 73, .	2.5	15
94	Temporal Variations of the Three Geomagnetic Field Components at Colaba Observatory around the Carrington Storm in 1859. Astrophysical Journal, 2022, 928, 32.	4.5	15
95	Turbulent microstructures and formation of folds in auroral breakup arc. Journal of Geophysical Research, 2011, 116, n/a-n/a.	3.3	14
96	A direct link between chorus emissions and pulsating aurora on timescales from milliseconds to minutes: A case study at subauroral latitudes. Journal of Geophysical Research: Space Physics, 2015, 120, 9617-9631.	2.4	14
97	Subauroral polarization streams: observations with the Hokkaido and King Salmon SuperDARN radars and modeling. Annales Geophysicae, 2008, 26, 3317-3327.	1.6	14
98	Self-consistent kinetic numerical simulation model for ring current particles in the Earth's inner magnetosphere. Journal of Geophysical Research, 2011, 116, n/a-n/a.	3.3	13
99	Ground-based multispectral high-speed imaging of flickering aurora. Geophysical Research Letters, 2011, 38, n/a-n/a.	4.0	13
100	Observed correlation between pulsating aurora and chorus waves at Syowa Station in Antarctica: A case study. Journal of Geophysical Research, 2012, 117, .	3.3	13
101	Sudden pressure enhancement and tailward retreat in the nearâ€Earth plasma sheet: THEMIS observation and MHD simulation. Journal of Geophysical Research: Space Physics, 2015, 120, 201-211.	2.4	13
102	Compound auroral micromorphology: ground-based high-speed imaging. Earth, Planets and Space, 2015, 67, 23.	2.5	13
103	Fast modulations of pulsating proton aurora related to subpacket structures of Pc1 geomagnetic pulsations at subauroral latitudes. Geophysical Research Letters, 2016, 43, 7859-7866.	4.0	13
104	Response of the incompressible ionosphere to the compression of the magnetosphere during the geomagnetic sudden commencements. Journal of Geophysical Research: Space Physics, 2016, 121, 1536-1556.	2.4	13
105	Cooperatives Roles of Dynamics and Topology in Generating the Magnetosphereâ€lonosphere Disturbances: Case of the Theta Aurora. Journal of Geophysical Research: Space Physics, 2018, 123, 9991.	2.4	13
106	Why does substorm-associated auroral surge travel westward?. Plasma Physics and Controlled Fusion, 2018, 60, 014024.	2.1	13
107	Variation of Radiation Belt Electron Flux During CME―and CIRâ€Driven Geomagnetic Storms: Van Allen Probes Observations. Journal of Geophysical Research: Space Physics, 2019, 124, 6524-6540.	2.4	13
108	Reproduction of Ground Magnetic Variations During the SC and the Substorm From the Global Simulation and Biot‣avart's Law. Journal of Geophysical Research: Space Physics, 2020, 125, e2019JA027172.	2.4	13

#	Article	lF	CITATIONS
109	Imaging cold ions in the plasma sheet from the Equatorâ€& satellite. Geophysical Research Letters, 2008, 35, .	4.0	12
110	Development of Magnetic Topology During the Growth Phase of the Substorm Inducing the Onset of the Nearâ€Earth Neutral Line. Journal of Geophysical Research: Space Physics, 2019, 124, 5158-5183.	2.4	12
111	Characteristics of CME―and CIRâ€Driven Ion Upflows in the Polar Ionosphere. Journal of Geophysical Research: Space Physics, 2019, 124, 3637-3649.	2.4	12
112	Space weather benchmarks on Japanese society. Earth, Planets and Space, 2021, 73, .	2.5	12
113	Simultaneous entry of oxygen ions originating from the Sun and Earth into the inner magnetosphere during magnetic storms. Journal of Geophysical Research, 2009, 114, .	3.3	11
114	Reimei observation of highly structured auroras caused by nonaccelerated electrons. Journal of Geophysical Research, 2010, 115, .	3.3	11
115	High-speed stereoscopy of aurora. Annales Geophysicae, 2016, 34, 41-44.	1.6	11
116	Theory, modeling, and integrated studies in the Arase (ERG) project. Earth, Planets and Space, 2018, 70, .	2.5	11
117	Energetic neutral atom images of a narrow flow channel from the plasma sheet: Astrid-1 observations. Journal of Geophysical Research, 2002, 107, SMP 5-1.	3.3	10
118	Decrease of auroral intensity associated with reversal of plasma convection in response to an interplanetary shock as observed over Zhongshan station in Antarctica. Journal of Geophysical Research, 2011, 116, .	3.3	10
119	Records of auroral candidates and sunspots in <i>Rikkokushi</i> , chronicles of ancient Japan from early 7th century to 887. Publication of the Astronomical Society of Japan, 2017, 69, .	2.5	10
120	Short-period mesospheric gravity waves and their sources at the South Pole. Atmospheric Chemistry and Physics, 2017, 17, 911-919.	4.9	10
121	Penetration of the electric fields of the geomagnetic sudden commencement over the globe as observed with the HF Doppler sounders and magnetometers. Earth, Planets and Space, 2021, 73, .	2.5	10
122	Magnetic Conjugacy of Pc1 Waves and Isolated Proton Precipitation at Subauroral Latitudes: Importance of Ionosphere as Intensity Modulation Region. Geophysical Research Letters, 2021, 48, e2020GL091384.	4.0	10
123	PSTEP: project for solar–terrestrial environment prediction. Earth, Planets and Space, 2021, 73, .	2.5	10
124	An interhemispheric comparison of GPS phase scintillation with auroral emission observed at the South Pole and from the DMSP satellite. Annals of Geophysics, 2013, 56, .	1.0	10
125	On the global production rates of energetic neutral atoms (ENAs) and their association with the Dst index. Geophysical Research Letters, 1999, 26, 2929-2932.	4.0	9
126	Characteristics of merging at the magnetopause inferred from dayside 557.7-nm all-sky images: IMF drivers of poleward moving auroral forms. Annales Geophysicae, 2006, 24, 3071-3098.	1.6	9

#	Article	IF	CITATIONS
127	Simultaneous groundâ€satellite optical observations of postnoon shock aurora in the Southern Hemisphere. Journal of Geophysical Research, 2009, 114, .	3.3	9
128	Displacement of conjugate points during a substorm in a global magnetohydrodynamic simulation. Journal of Geophysical Research, 2011, 116, n/a-n/a.	3.3	9
129	Further evidence for a connection between auroral kilometric radiation and groundâ€level signals measured in Antarctica. Journal of Geophysical Research: Space Physics, 2015, 120, 2061-2075.	2.4	9
130	Response of ionospheric electric fields at midâ€low latitudes during sudden commencements. Journal of Geophysical Research: Space Physics, 2015, 120, 4849-4862.	2.4	9
131	Transient ionization of the mesosphere during auroral breakup: Arase satellite and ground-based conjugate observations at Syowa Station. Earth, Planets and Space, 2019, 71, .	2.5	9
132	Intense Geomagnetic Storm during Maunder Minimum Possibly by a Quiescent Filament Eruption. Astrophysical Journal, 2019, 887, 7.	4.5	9
133	The Extreme Space Weather Event in 1941 February/March. Astrophysical Journal, 2021, 908, 209.	4.5	9
134	The Intensity and Evolution of the Extreme Solar and Geomagnetic Storms in 1938 January. Astrophysical Journal, 2021, 909, 197.	4.5	9
135	The extreme solar and geomagnetic storms on 1940 March 20–25. Monthly Notices of the Royal Astronomical Society, 2022, 517, 1709-1723.	4.4	9
136	Dayside proton aurora associated with magnetic impulse events: South Pole observations. Journal of Geophysical Research, 2010, 115, .	3.3	8
137	Fine-scale dynamics of black auroras obtained from simultaneous imaging and particle observations with the Reimei satellite. Journal of Geophysical Research, 2011, 116, n/a-n/a.	3.3	8
138	Evolution of the current system during solar wind pressure pulses based on aurora and magnetometer observations. Earth, Planets and Space, 2016, 68, .	2.5	8
139	First evidence of patchy flickering aurora modulated by multiâ€ion electromagnetic ion cyclotron waves. Geophysical Research Letters, 2017, 44, 3963-3970.	4.0	8
140	Propagation and evolution of electric fields associated with solar wind pressure pulses based on spacecraft and groundâ€based observations. Journal of Geophysical Research: Space Physics, 2017, 122, 8446-8461.	2.4	8
141	Impact of substorm time O <sup>+</sup> outflow on ring current enhancement. Journal of Geophysical Research: Space Physics, 2017, 122, 6304-6317.	2.4	8
142	Magnetosphereâ€ŀonosphere Convection Under the Due Northward IMF. Journal of Geophysical Research: Space Physics, 2019, 124, 6812-6832.	2.4	8
143	The Celestial Sign in the Anglo-Saxon Chronicle in the 770s: Insights on Contemporary Solar Activity. Solar Physics, 2019, 294, 1.	2.5	8
144	Effects of the IMF Direction on Atmospheric Escape From a Marsâ€like Planet Under Weak Intrinsic Magnetic Field Conditions. Journal of Geophysical Research: Space Physics, 2021, 126, e2020JA028485.	2.4	8

#	Article	IF	CITATIONS
145	Dual source populations of substorm-associated ring current ions. Annales Geophysicae, 2009, 27, 1431-1438.	1.6	7
146	Energy-dependent evolution of ring current protons during magnetic storms. Journal of Geophysical Research, 2011, 116, n/a-n/a.	3.3	7
147	Electron properties in invertedâ€V structures and their vicinities based on Reimei observations. Journal of Geophysical Research: Space Physics, 2014, 119, 3650-3663.	2.4	7
148	Quasi-periodic rapid motion of pulsating auroras. Polar Science, 2016, 10, 183-191.	1.2	7
149	An Analysis of Trouvelot's Auroral Drawing on 1/2 March 1872: Plausible Evidence for Recurrent Geomagnetic Storms. Journal of Geophysical Research: Space Physics, 2020, 125, e2020JA028227.	2.4	7
150	Structure and dynamics of the proton energy density in the inner magnetosphere. Advances in Space Research, 2004, 33, 711-718.	2.6	6
151	Outflowing protons and heavy ions as a source for the sub-keV ring current. Annales Geophysicae, 2009, 27, 839-849.	1.6	6
152	Ion drift simulation of sudden appearance of sub-keV structured ions in the inner magnetosphere. Annales Geophysicae, 2014, 32, 83-90.	1.6	6
153	Simulation study of near-Earth space disturbances: 1. magnetic storms. Progress in Earth and Planetary Science, 2019, 6, .	3.0	6
154	Simulation study of near-Earth space disturbances: 2. Auroral substorms. Progress in Earth and Planetary Science, 2019, 6, .	3.0	6
155	Signatures of substorm related overshielding electric field at equatorial latitudes under steady southward IMF Bz during main phase of magnetic storm. Advances in Space Research, 2019, 64, 1975-1988.	2.6	6
156	Formation and Release of the Harang Reversal Relating With the Substorm Onset Process. Journal of Geophysical Research: Space Physics, 2021, 126, .	2.4	6
157	Magnetospheric solitary structure maintained by 3000 km/s ions as a cause of westward moving auroral bulge at 19 MLT. Annales Geophysicae, 2009, 27, 2947-2969.	1.6	6
158	Roles of the Mâ€I Coupling and Plasma Sheet Dissipation on the Growthâ€Phase Thinning and Subsequent Transition to the Onset. Journal of Geophysical Research: Space Physics, 2021, 126, .	2.4	6
159	Formation and evolution of highâ€plasmaâ€pressure region in the nearâ€Earth plasma sheet: Precursor and postcursor of substorm expansion onset. Journal of Geophysical Research: Space Physics, 2015, 120, 6427-6435.	2.4	5
160	Fastâ€moving diffuse auroral patches: A new aspect of daytime Pc3 auroral pulsations. Journal of Geophysical Research: Space Physics, 2017, 122, 1542-1554.	2.4	5
161	Sporadic auroras near the geomagnetic equator: in the Philippines, on 27 October 1856. Annales Geophysicae, 2018, 36, 1153-1160.	1.6	5
162	On the Driver of Daytime Pc3 Auroral Pulsations. Geophysical Research Letters, 2019, 46, 553-561.	4.0	5

#	Article	IF	CITATIONS
163	Candidate Auroral Observations Indicating a Major Solar–Terrestrial Storm in 1680: Implication for Space Weather Events during the Maunder Minimum. Astrophysical Journal, 2021, 909, 29.	4.5	5
164	Daytime Pc5 Diffuse Auroral Pulsations and Their Association With Outer Magnetospheric ULF Waves. Journal of Geophysical Research: Space Physics, 2021, 126, e2021JA029218.	2.4	5
165	Flux Enhancement of Relativistic Electrons Associated with Substorms. , 2016, , 333-353.		5
166	Where Is Region 1 Fieldâ€Aligned Current Generated?. Journal of Geophysical Research: Space Physics, 2022, 127, .	2.4	5
167	A review for Japanese auroral records on the three extreme space weather events around the International Geophysical Year (1957–1958). Geoscience Data Journal, 2023, 10, 142-157.	4.4	5
168	Reply [to "Comment on "Simulation study on fundamental properties of the storm-time ring current― by Y. Ebihara and M. Ejiriâ€]. Journal of Geophysical Research, 2001, 106, 6323-6324.	3.3	4
169	Spatial characteristics of wave-like structures in diffuse aurora obtained using optical observations. Annales Geophysicae, 2012, 30, 1693-1701.	1.6	4
170	Poleward moving auroral arcs observed at the South Pole Station and the interpretation by field line resonances. Journal of Geophysical Research, 2012, 117, .	3.3	4
171	Void structure of O <sup>+</sup> ions in the inner magnetosphere observed by the Van Allen Probes. Journal of Geophysical Research: Space Physics, 2016, 121, 11,698.	2.4	4
172	Evolution of auroral substorm as viewed from MHD simulations: dynamics, energy transfer and energy conversion. Reviews of Modern Plasma Physics, 2020, 4, 1.	4.1	4
173	How Do Auroral Substorms Depend on Earth's Dipole Magnetic Moment?. Journal of Geophysical Research: Space Physics, 2021, 126, .	2.4	4
174	Occurrence Distribution of Polar Cap Patches: Dependences on UT, Season and Hemisphere. Journal of Geophysical Research: Space Physics, 2021, 126, .	2.4	4
175	Global Simulation of the Jovian Magnetosphere: Transitional Structure From the Io Plasma Disk to the Plasma Sheet. Journal of Geophysical Research: Space Physics, 2021, 126, e2021JA029232.	2.4	4
176	Single particle simulation on the storm-time ring current formation and DST variation. Advances in Space Research, 2003, 31, 1051-1058.	2.6	3
177	Interhemispheric observations of field line resonance frequencies as a continuous function of ground latitude in the auroral zones. Polar Science, 2008, 2, 73-86.	1.2	3
178	Fineâ€scale transient arcs seen in a shock aurora. Journal of Geophysical Research: Space Physics, 2014, 119, 6249-6255.	2.4	3
179	Simulation of substormâ€ŧime acceleration of oxygen ions on azimuthally directed magnetic field lines in the nearâ€Earth plasma sheet. Journal of Geophysical Research: Space Physics, 2014, 119, 6167-6176.	2.4	3
180	Nonlinear Wave Growth Analysis of Whistlerâ€Mode Chorus Generation Regions Based on Coupled MHD and Advection Simulation of the Inner Magnetosphere. Journal of Geophysical Research: Space Physics, 2020, 125, e2019JA026951.	2.4	3

#	Article	IF	CITATIONS
181	Spatial Evolution of Waveâ€Particle Interaction Region Deduced From Flashâ€Type Auroras and Chorusâ€Ray Tracing. Journal of Geophysical Research: Space Physics, 2021, 126, e2021JA029254.	2.4	3
182	Development of the substorm as a manifestation of convection transient. Journal of Geophysical Research: Space Physics, 2021, 126, e2020JA028942.	2.4	3
183	Dense ion clouds of 0.1 â^ 2 keV ions inside the CPS-region observed by Astrid-2. Annales Geophysicae, 2001, 19, 621-631.	1.6	3
184	Reproducibility of the Geomagnetically Induced Currents at Middle Latitudes During Space Weather Disturbances. Frontiers in Astronomy and Space Sciences, 2021, 8, .	2.8	3
185	Slow Contraction of Flash Aurora Induced by an Isolated Chorus Element Ranging From Lowerâ€Band to Upperâ€Band Frequencies in the Source Region. Geophysical Research Letters, 2022, 49, .	4.0	3
186	Japanese polar patrol balloon experiments from 2002 to 2004. Advances in Space Research, 2006, 37, 2043-2051.	2.6	2
187	Optical and particle observations of type B red aurora. Geophysical Research Letters, 2009, 36, .	4.0	2
188	Fine-Scale Characteristics of Black Aurora and its Generation Process. Geophysical Monograph Series, 0, , 271-278.	0.1	2
189	Generation of largeâ€amplitude electric field and subsequent enhancement of O + ion flux in the inner magnetosphere during substorms. Journal of Geophysical Research: Space Physics, 2015, 120, 4825-4840.	2.4	2
190	Formation of multiple energy dispersion of H <sup>+</sup> , He <sup>+</sup> , and O <sup>+</sup> ions in the inner magnetosphere in response to interplanetary shock. Journal of Geophysical Research: Space Physics, 2017, 122, 4387-4397.	2.4	2
191	Evolution of Pitch Angleâ€Distributed Megaelectron Volt Electrons During Each Phase of the Geomagnetic Storm. Journal of Geophysical Research: Space Physics, 2020, 125, e2019JA027086.	2.4	2
192	Asymmetric Development of Auroral Surges in the Northern and Southern Hemispheres. Geophysical Research Letters, 2020, 47, e2020GL088750.	4.0	2
193	The extreme space weather events in October 1788. Publication of the Astronomical Society of Japan, 2021, 73, 1367-1374.	2.5	2
194	The fate of O <sup>+</sup> ions observed in the plasma mantle: particle tracing modelling and cluster observations. Annales Geophysicae, 2020, 38, 645-656.	1.6	2
195	Superposed epoch analyses of geoelectric field disturbances in Japan in response to different geomagnetic activities. Space Weather, 0, , .	3.7	2
196	Instantaneous Achievement of the Hall and Pedersen–Cowling Current Circuits in Northern and Southern Hemispheres During the Geomagnetic Sudden Commencement on 12 May 2021. Frontiers in Astronomy and Space Sciences, 2022, 9, .	2.8	2
197	Correction to "Ring current and the magnetosphere-ionosphere coupling during the superstorm of 20 November 2003â€. Journal of Geophysical Research, 2005, 110, .	3.3	1
198	Microburst cusp ion precipitation observed with Reimei. Journal of Geophysical Research, 2008, 113, .	3.3	1

#	ARTICLE	IF	CITATIONS
199	Oscillations of the equatorward boundary of the ion auroral oval – radar observations. Journal of Geophysical Research, 2008, 113, .	3.3	1
200	Ion-dispersion and rapid electron fluctuations in the cusp: a case study. Annales Geophysicae, 2008, 26, 2485-2502.	1.6	1
201	Energy Flow in the Region 2 Fieldâ€Aligned Current Region Under Quasiâ€steady Convection. Journal of Geophysical Research: Space Physics, 2020, 125, e2019JA026998.	2.4	1
202	Great "Space Weather Events―in March 1653 and September 1672 Were Not Supported With Simultaneous/Clustering Auroral Observations During the Maunder Minimum. Frontiers in Astronomy and Space Sciences, 2022, 9, .	2.8	1
203	Locations of proton isotropic boundaries as measured by conjugate high-altitude and low-altitude satellites. Advances in Space Research, 2003, 31, 1265-1270.	2.6	Ο
204	The Gattini South Pole UV experiment. , 2012, , .		0
205	Ground-based observations of hiss-like emissions changed from chorus emissions and related pulsating aurora. , 2014, , .		Ο
206	Threeâ€Dimensional Closure of Fieldâ€Aligned Currents in the Polar Ionosphere. Journal of Geophysical Research: Space Physics, 2021, 126, e2021JA029421.	2.4	0
207	Spatiotemporal development of pulsating auroral patch associated with discrete chorus elements: Arase and PWING observations. , 2019, , .		Ο
208	Mechanism of Auroral Breakup. Japanese Journal of Multiphase Flow, 2019, 33, 267-274.	0.3	0
209	Characterization of the Measured Events. , 0, , .		0
210	Further Search for Extreme Events. , 0, , .		0
211	Poleward Moving Auroral Arcs and Pc5 Oscillations. Journal of Geophysical Research: Space Physics, 2022, 127, .	2.4	О